Virology 481 (2015) 113–123

Contents lists available at ScienceDirect

Virology

journal homepage: www.elsevier.com/locate/yviro

Molecular characterization of *Pvr9* that confers a hypersensitive response to *Pepper mottle virus* (a potyvirus) in *Nicotiana benthamiana*

Phu-Tri Tran [a,b], Hoseong Choi [a,b], Doil Choi [b,c,d], Kook-Hyung Kim [a,b,d,*]

[a] Department of Agricultural Biotechnology, College of Agriculture and Life Sciences, Seoul National University, Seoul 151-921, Republic of Korea
[b] Plant Genomics and Breeding Institute, College of Agriculture and Life Sciences, Seoul National University, Seoul 151-921, Republic of Korea
[c] Department of Plant Science, College of Agriculture and Life Sciences, Seoul National University, Seoul 151-921, Republic of Korea
[d] Research Institute of Agriculture and Life Sciences, College of Agriculture and Life Sciences, Seoul National University, Seoul 151-921, Republic of Korea

ARTICLE INFO

Article history:
Received 30 December 2014
Returned to author for revisions
31 January 2015
Accepted 26 February 2015
Available online 14 March 2015

Keywords:
Resistance gene
Pepper mottle virus
Pvr9
Hypersensitive response
Elicitor
NIb

ABSTRACT

There are some *R* genes against potyviruses which were mapped in pepper. However, none of them has been characterized at the molecular level. In this study, we characterized *Pvr9* which is an *Rpi-blb2* ortholog from pepper and confers a hypersensitive response to *Pepper mottle virus* (PepMoV) in a transient expression system in *Nicotiana benthamiana*. This gene putatively encoded for 1298 amino acids and is located on pepper chromosome 6. PepMoV NIb was the elicitor of the *Pvr9*-mediated hypersensitive response. NIb from several other potyviruses also elicited the hypersensitive response. Inoculation of pepper with PepMoV resulted in a minor increase in *Pvr9* transcription in the resistant cultivar CM334 and a slight down-regulation in the susceptible cultivar Floral Gem. The 5′ upstream region of *Pvr9* from cultivar CM334 had higher transcription activity than the region from cultivar Floral Gem. The cultivars CM334 and Floral Gem had non-functional *Pvr9* homologs with loss-of-function mutations.

Introduction

In plants, gene-mediated resistance is one of the defense mechanisms that prevents or reduces virus infection (Kang et al., 2005). Based on their mode of inheritance, plant resistance genes are classified as recessive or dominant. Recessive resistance genes provide a passive resistance in which virus multiplication is compromised by the incompatible interactions between the virus and host factors, most of which are variants of eukaryotic translation initiation factors eIF4e (Diaz-Pendon et al., 2004). Dominant resistance genes (*R* genes), in contrast, confer an active resistance by encoding resistance proteins (R proteins) that recognize pathogen effectors or so-called avirulence (*Avr*) factors (Chisholm et al., 2006). *R* genes usually encode proteins with a nucleotide-binding site (NBS) and a leucine-rich repeat (LRR) region (Ellis et al., 2000). The NBS domain comprises a functional nucleotide-binding pocket capable of binding and hydrolyzing ATP (Tameling et al., 2002) and is responsible for signaling resistant responses (Rairdan and Moffett, 2006). The LRR domain is made up of individual repeats with the consensus leucine rich repeat motif and was proven to be involved in Avr recognition (Ellis et al., 2007). These NBS-LRR proteins are classified into two groups: the TIR-NBS-LRR proteins contain an N-terminal domain with Toll/Interleukin-1 receptor homology, and the CC-NBS-LRR proteins are characterized by an N-terminal coiled-coil motif (Dangl and Jones, 2001).

Several members of the genus *Potyvirus* are highly destructive pathogens of pepper plants (*Capsicum* sp.) (Moury et al., 2005; Nelson and Wheeler, 1978). In turn, pepper plants carry potyvirus resistance genes, most of which are recessive. *pvr1* confers broad-spectrum recessive resistance to *Tobacco etch virus* (TEV), *Pepper mottle virus* (PepMoV), and *Potato virus Y* (PVY) in *Capsicum chinense* 'PI 152225' and 'PI 169326' (Greenleaf 1956, 1986; Murphy et al., 1998). Potyvirus resistance alleles have also been found at a second locus, *pvr2*. The allele *pvr2*^{1} of *Capsicum annuum* 'Yolo RP10' and 'Yolo Y' controls the recessive resistance to PVY pathotype 0 (Cook, 1960; Gebre Selassie et al., 1983). The allele *pvr2*^{2} from *C. annuum* 'PI 264281', 'SC46252', and 'Florida VR2' confers recessive resistance to PVY pathotype 1 and TEV (Cook and Anderson, 1959; Gebre Selassie et al., 1983). In addition, polygenic resistance to PVY consisting of a combination of quantitative trait loci was found at locus *pvr2* in *C. annuum* 'Perennial' (Caranta et al., 1997). A third locus, *pvr3*, contains a monogenic recessive gene in *C. annuum* 'Avelar', which is resistant to PepMoV (Kyle and Palloix, 1997; Zitter and Cook, 1973). The recessive loci *pvr5 and pvr8* from *C. annuum* 'Criollo de Morelos 334' (CM334) provide resistance to PVY pathotype 0 and pathotype 1 isolate P-62-81, respectively (Andrés et al., 2004; Dogimont et al., 1996). A

* Corresponding author at: Department of Agricultural Biotechnology, College of Agriculture and Life Sciences, Seoul National University, Seoul 151-921, Republic of Korea.
E-mail address: kookkim@snu.ac.kr (K.-H. Kim).

http://dx.doi.org/10.1016/j.virol.2015.02.052
0042-6822/

recessive gene *pvr6*, which is complementary with $pvr2^2$ for resistance to *Pepper veinal mottle virus* (PVMV), was found in *C. annuum* 'Perennial' (Caranta et al., 1996).

There are only a few pepper *R* genes against potyviruses. The dominant gene *Pvr4* from *C. annuum* CM334 confers a broad spectrum and extreme resistance to potyviruses (Dogimont et al., 1996). The *R* gene *Pvr7* from *C. chinense* 'PI 159236' is tightly linked to *Pvr4* on chromosome 10 and confers a hypersensitive response to *Pepper mottle virus* (PepMoV) Florida (V1182) strain (Grube et al., 2000). Recently, a novel codominant molecular marker for an *R* gene that confers resistance to *Chilli veinal mottle virus* (potyvirus, ChiVMV) was mapped on chromosome 6 of *C. annuum* "NW4" (Lee et al., 2013). However, none of these *R* genes has been cloned or characterized at the molecular level.

We previously screened for genes that confer resistance to viruses based on virus inoculation and transient over-expression of candidate *R* genes by agroinfiltration in *Nicotiana benthamiana*; using this method, we isolated an *Rpi-blb2* ortholog (named the *Pvr9* gene) that confers a hypersensitive response to PepMoV in *N. benthamiana* (Tran et al., 2014). Here, we determined the molecular characteristics of the *Pvr9* gene and its elicitor. We showed that this *R* gene putatively encodes for 1298 amino acids of a possible CC-NBS-LRR protein and was predicted to be located on pepper chromosome 6. We also showed that PepMoV NIb is the elicitor of the *Pvr9*-mediated hypersensitive response. Finally, we used mutational analyses to identify the amino acid residues that are important to the function of both the *R* gene and the elicitor.

Results

Pvr9 characterization

According to the accepted proposed revision of nomenclature for potyvirus resistance genes in *Capsicum* (Kyle and Palloix, 1997), the pepper *Rpi-blb2* ortholog that confers a hypersensitive response to PepMoV in *N. benthamiana* was designated *Pvr9*. The response caused by *Pvr9* upon PepMoV infection was confirmed in the current study by agroinfiltration of *Pvr9* and PepMoV inoculation in *N. benthamiana* as described previously (Tran et al., 2014). Two days after agroinfiltration, a hypersensitive response on infiltrated leaves was detected by trypan blue staining (Fig. 1A, left panel). The accumulation of H_2O_2, the hallmark of the hypersensitive response (Levine et al., 1994), was detected by DAB staining (Fig. 1A, right panel).

The coding sequence of *Pvr9* was determined from the transiently expressed transcripts of *Pvr9* in *N. benthamiana* leaves. By RT-PCR, cloning, and sequencing, an open reading frame of 3897 nucleotides was identified. Sequence alignment of the mRNA and genomic DNA revealed an intron from nucleotide 43 to nucleotide 169 of the genomic sequence (Fig. 1B, upper panel). This open reading frame putatively encodes 1298 amino acids (Fig. 1B, lower panel). Domain and motif searching (Jones et al., 2014) detected an NBS domain from amino acid residue 566 to residue 843 (Fig. 1B, green box in lower panel), which included motifs of kinase-1a (known as the P-loop or Walker A with motif GxxxxGKS/T, in which x indicates any residue), kinase-2 (known as the Walker B with motif hhhhDD/E, in which h is mostly a hydrophobic residue), kinase 3a (motif hhhhToR, in which o is an alcoholic residue), and a hydrophobic domain (GPLP motif). LRR motif scanning (Bej et al., 2014) revealed an LRR domain from residue 1005 to residue 1241 (Fig. 1B, yellow box in lower panel) with at least five leucine-rich repeat (motif LxxLxLxxNxL, in which L is Leu/Ile/Val/Phe and N is Asn/Thr/Ser/Cys). There is a possible CC domain from residue 443 to residue 535 (Fig. 1B, white box in lower panel) including a possible leucine zipper and a heptad repeat before the NBS domain. Thus, these analyses suggested that *Pvr9* belongs to the CC-NBS-LRR class.

The physical position of *Pvr9* in the pepper genome was predicted by nucleotide blasting against chromosome data sets of the pepper genome database (http://cab.pepper.snu.ac.kr/). The highest homologous sequences ($>99\%$) of 4041 base pairs belonged to chromosome 6 in pepper *C. annuum* Zunla-1 and *C. annuum* var. *grabriusculum*. They were determined to be located from nucleotide 213,329,659 to nucleotide 213,326,619 of *C. annuum* Zunla-1 chromosome 6 and from nucleotide 195,062,197 to nucleotide 195,058,157 of *C. annuum* var. *grabriusculum* chromosome 6. In Fig. 1C, the position of *Pvr9* on pepper chromosome 6 is schematically represented relative to the previously published markers C2At3g25120, C2At2g39690, C2At3g46780, and CVMV-3 (Lee et al., 2013; Wu et al., 2009).

The relationship of Pvr9 with other characterized plant resistance proteins was revealed by NCBI protein blasting using deduced Pvr9 amino acid sequences. These homologous proteins belong to the CC-NBS-LRR class and originate from peppers (*C. annuum* and *Capsicum chacoense*), tomatoes (*Solanum lycopersicum* and *Solanum pimpinellifolium*), potatoes (*Solanum bulbocastanum, Solanum desmissum,* and *Solanum tuberosum*), and *Arabidopsis thaliana*. The genes encoding the homologous sequences include *Rpi-blb2* (accession no. DQ122125), *Mi-1* (AF091048), *Mi-1.1* (NM_001247693), *Mi-1.2* (NM_001247134), *CaMi* (DQ465824), *CaMe* (FJ231739), *Hero* (AJ457051), *SW-5F* (JX026925), *SW-5B* (AY007366), *PRF* (U65391), *Prf* (AF220602), *R1* (AAL39063), *BS2* (AF202179), *Gpa2* (AJ249449), *Rx* (AJ011801), RGC1 (AF266747), *RCY1* (AB087829), *HRT* (AF234174), *RPP8* (AF089710), and *I2* (AF118127). By using the neighbor joining method with MEGA6 software, an unrooted and scaled phylogenetic tree was constructed from putative amino acid sequences of Pvr9 and the other functional R proteins (Fig. 1D). The analysis showed that Pvr9, Rp-blb2, and nematode resistance proteins (CaMe, Mi-1, Mi-1.1, Mi-1.2, and CaMi) formed a monophyletic clade; Pvr9 was closest to CaMe, the nematode resistance protein in pepper.

Elicitor identification and characterization

To determine which PepMoV gene triggers the hypersensitive response mediated by *Pvr9*, we cloned the viral genes from PepMoV isolate 134 (Fig. 2A) (Kim et al., 2009) in the modified vector pPZP212 and transformed the cloned genes into *Agrobacterium*. The transformants of individual viral gene and *Pvr9* were then co-infiltrated into *N. benthamiana*. As shown in Fig. 2B, co-agroinfiltration of transformants expressing *NIb* and *Pvr9* triggered a hypersensitive response but co-infiltration of the other transformants did not. This demonstrated that PepMoV NIb is the elicitor of the hypersensitive response. However, direct interaction between the *NIb* and *Pvr9* was not found in yeast two hybrid and bimolecular fluorescent complementation assay (Supplementary Fig. S1).

To determine whether other potyvirus NIbs elicit a response from Pvr9, the *NIb* gene from PVY, *Potato virus A* (PVA), *Turnip mosaic virus* (TuMV), *Soybean mosaic virus* (SMV), and *Zucchini yellow mosaic virus* (ZYMV) were cloned to the modified pPZP212. Co-agroinfiltration of these transformants expressing other potyvirus NIbs with Pvr9 showed that the *NIbs* from PVY, PVA, and TuMV triggered the hypersensitive response. However, the ZYMV *NIb* triggered only a weak hypersensitive response, and the SMV *NIb* failed to trigger a hypersensitive response (Fig. 3A). To explore the phylogenetic relationships among these NIb proteins, we generated an unrooted and scaled phylogenetic tree from the NIb amino acid sequences of potyviruses. As shown in Fig. 3B, the NIbs of PepMoV, PVY, and PVA belonged to a monophyletic group, and the NIbs of ZYMV and SMV belonged to another clade. Branching of the phylogenetic tree which is usually interpreted as a specification event in phylogenetics, especially at the early

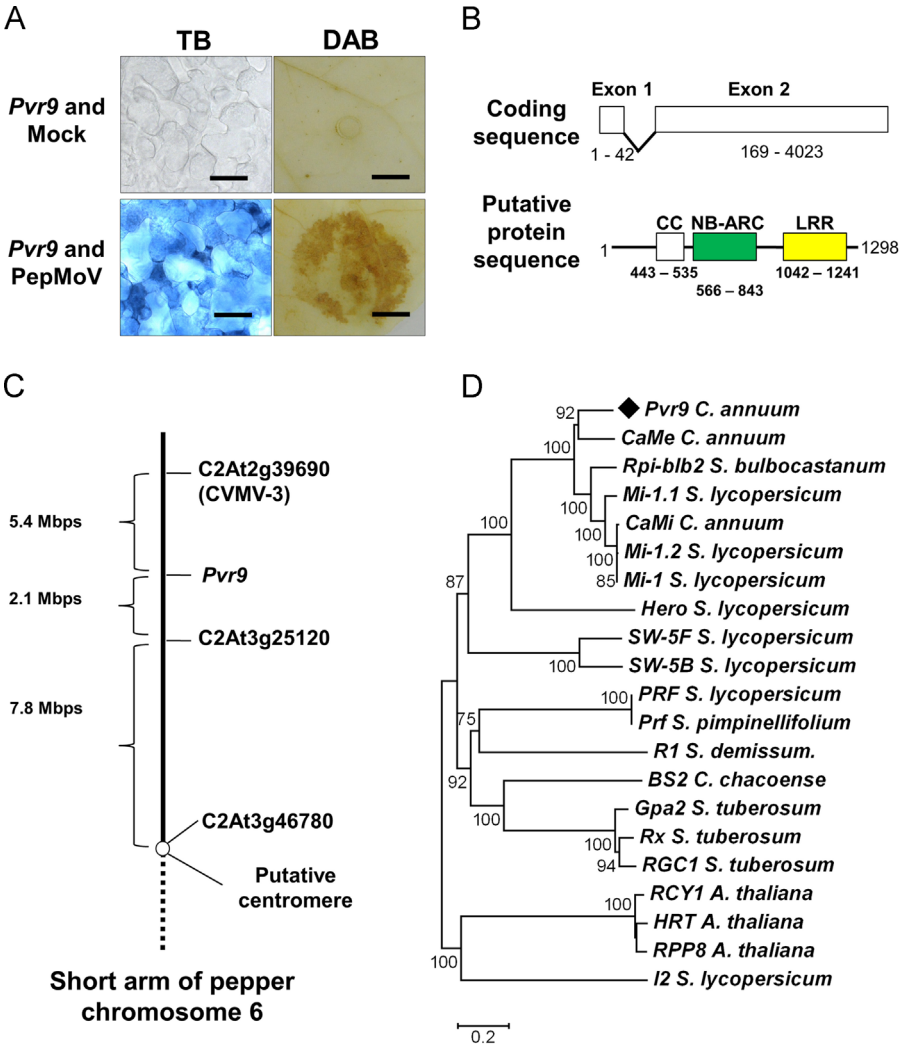

Fig. 1. *Pvr9* characterization. (A) Responses of *Pvr9* to mock inoculation (*Pvr9* and Mock) or PepMoV inoculation (*Pvr9* and PepMoV) in *N. benthamiana* as indicated by trypan blue staining (TB, left panel, scale bar = 50 μm) and DAB staining (DAB, right panel, scale bar = 5 mm). (B) The upper diagram indicates the representative structure of the *Pvr9* coding sequence, which includes two exons and one intron (numbers indicate nucleotide position from the start codon); the lower diagram indicates the representative structure of the Pvr9 putative protein, which includes a possible coiled-coil domain (CC), a nucleotide-binding domain (NB-ARC), and a leucine-rich repeat domain (LRR) (the number indicates the amino acid position from the N terminal). (C) Predicted relative position of *Pvr9* on the short arm of pepper chromosome 6 with COSII markers C2At2g39690 (CVMV-3), C2At3g25120, and C2At3g46780. (D) Phylogenetic tree of Pvr9 and other characterized R proteins; species names of the plants from which the R gene were isolated are indicated in italics; scale bar indicates 0.2 substitutions per amino acid position; the bootstrap values expressed as a percentage of 1000 replicates are indicated at each node.

nodes (Fig. 3B), revealed that the NIb of TuMV shared a common ancestor with the NIb of PepMoV rather than with the NIbs of ZYMV and SMV.

Mapping of the elicitor interaction domain

To find those portions of the NIb protein that are required to elicit the Pvr9 response, several truncated mutants were generated by deletions from the two ends of PepMoV NIb. Truncated mutants that lacked amino acid residues 1–185 (NIbΔ(1–185)) and residues 445 to 517 (NIbΔ(445–517)) still triggered the Pvr9 response. However, the truncated mutants lacking amino acid residues 1 to 235 and residues 370–517 failed to trigger a response (Fig. 4A, NIbΔ(1–235) and NIbΔ(370–519), respectively). These results suggested that the residues 186–235 and residues 370–445 are important for NIb elicitor activity. In support of this inference, internal deletion mutants lacking the residues 186–235 and 370–445 elicited no Pvr9 response or a greatly attenuated response while the mutant lacking 236–396 still triggered the Pvr9 response (Fig. 4B; NIbΔ(186–235), NIbΔ(370–445), and NIbΔ(236–369)). To confirm the role of these regions in eliciting the Pvr9 response, we constructed chimeras by replacing the residues 186–235, residues 370–445, or both of these regions of SMV *NIb* with the corresponding PepMoV regions (Fig. 4C). As shown in Fig. 4D, the double replacement (SMV–NIb hybrid 3) caused SMV NIb to trigger the Pvr9 response while the single replacements (SMV–NIb hybrid 1 and hybrid 2) did not.

Expression of Pvr9 in susceptible and resistant pepper cultivars in response to PepMoV infection

Transcription patterns of *Pvr9* were monitored in pepper cultivars *C. annuum* Floral Gem and *C. annuum* CM334, which are susceptible and resistant, respectively, to PepMoV (Dogimont et al., 1996). First, tissues from the inoculated plants were collected, and total RNAs were extracted before inoculation (day 0) and after inoculation (from day 1 to day 15). Infectivity of PepMoV was then checked by symptom observation and real-time RT-PCR (qRT-PCR) with PepMoV CP-specific primers. The transcription level of *Pvr9* was assessed by qRT-PCR with the reference gene *GAPDH*.

Following inoculation, leaf stunting was evident at 7 dpi (days after inoculation) and yellowing was evident at 15 dpi in Floral Gem but not in CM334 (Fig. 5A). The qRT-PCR signals representing PepMoV CP transcripts increased in Floral Gem but not in CM334 (Fig. 5B). In Floral Gem, the signal logarithmically increased in inoculated (local) leaves and drastically increased in upper leaves (systemic) after 5 dpi. However, the signal decreased in both local and systemic leaves of CM334 (except for a slight increase in local leaves by 3 dpi). *Pvr9* transcript levels were generally stable in the upper leaves of both pepper cultivars (Fig. 5C and D, line graphs).

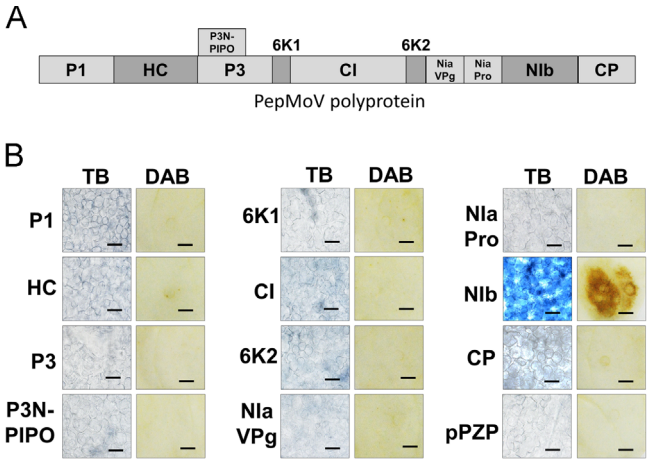

Fig. 2. Identification of the elicitor of *Pvr9*. (A) Representative map depicts PepMoV polyprotein with different premature products (P1, HC, P3, 6K1, CI, 6K2, NIa, NIb, and CP). (B) Responses of *Pvr9* to different PepMoV genes at 2 days after co-agroinfiltration; the empty modified pPZP212 vector was used as a control; the hypersensitive response and H_2O_2 were indicated by trypan blue staining (TB, left panel, scale bar=50 μm) and DAB staining (DAB, right panel, scale bar=5 mm), respectively.

In virus-inoculated leaves of CM334, the *Pvr9* transcript level increased slightly from 2 to 10 dpi in comparison to mock inoculation (Fig. 5C, white and grey bars). In Floral Gem, however, *Pvr9* transcription was not induced by PepMoV inoculation; at some time points (1, 3, 10, and 15 dpi), the transcript levels were lower in PepMoV-inoculated leaves than in mock-inoculated leaves (Fig. 5D, white and grey bars).

Transcription of a gene is usually affected by upstream regulatory sequences. This could contribute to the susceptibility and differential expression patterns of *Pvr9* among the tested pepper cultivars. To find the promoter sequence of *Pvr9*, 10.3-kb upstream sequences of *Pvr9* were isolated by chromosome walking and PCRs from Floral Gem and CM334 pepper. These sequences were fused to GFP and cloned into modified promoterless GFP-pCAMBIA 0380 (Fig. 6A). *Agrobacterium*-mediated transient expression showed that the sequence from CM334 induced expression of GFP at 2 days after agroinfiltration (Fig. 6B). The sequence from pepper Floral Gem induced a weak expression of GFP that was detectable by qRT-PCR. The level of GFP transcription driven by the *Pvr9* upstream sequence was about 5-fold higher for CM334 than for Floral Gem (Fig. 6C).

Important amino acid residues for Pvr9 function

From pepper cultivar Floral Gem, we isolated a variant of *Pvr9*, named homolog 1. Since only one copy of *Pvr9* was found in pepper chromosomal databases (http://cab.pepper.snu.ac.kr/), the homolog 1 could locate in same locus with *Pvr9* but in the paired chromosome. The amino acid alignment between Pvr9 and homolog 1 showed that homolog 1 had an insertion of six amino acids between residue 6 and 7, and 16 substitutions (Supplementary Fig. S2).The 8 substitutions and an insertion of 6 amino acids at 5′ and 3′ end are probably from primer design for isolation of *Pvr9* because this gene is cloned with degenerative primers (Tran et al., 2014). Co-agroinfiltration of

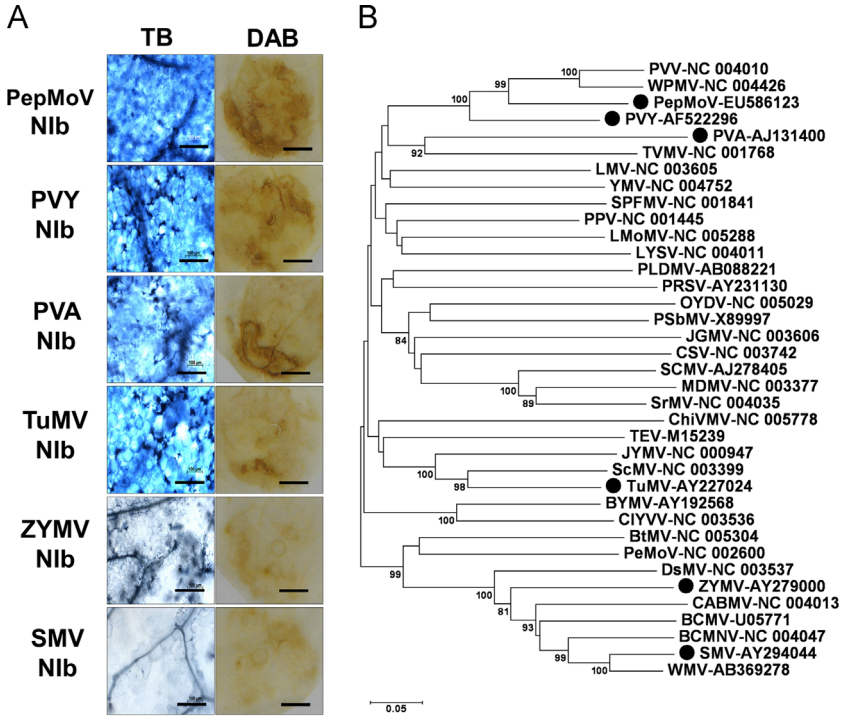

Fig. 3. Pvr9 response to several potyvirus NIbs and phylogenetic tree of potyvirus NIbs. (A) Responses of Pvr9 to PepMoV–NIb, PVY–NIb, PVA–NIb, TuMV–NIb, ZYMV–NIb, and SMV–NIb as indicated by trypan blue staining (TB, left panel, scale bar=200 μm) and DAB staining (DAB, right panel, scale bar=1 cm). (B) Phylogenetic tree of NIbs from potyviruses; an unrooted and scaled phylogenetic tree was constructed from putative amino acid sequences of NIbs from potyviruses; black dots in the phylogenetic tree indicate positions of the tested NIbs; scale bar indicates 0.05 substitutions per amino acid position; the bootstrap values expressed as percentage of 1000 replicates are indicated at each node (70% cut off).

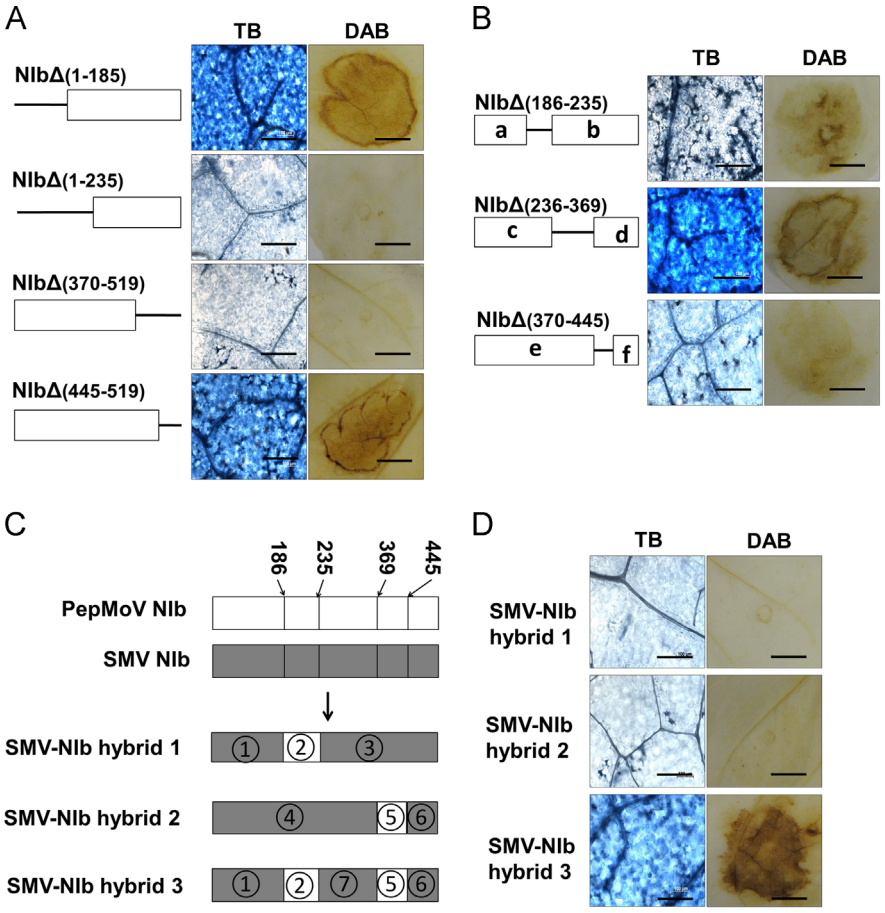

Fig. 4. Characterization of the NIb elicitor. (A) Responses of *Pvr9* to different *NIb* fragments, which were truncated from the N terminal (NIbΔ(1–185), NIbΔ(1–235)) or from the C terminal (NIbΔ(370–519) and NIbΔ(445–519)); the numbers in parentheses indicate the amino acid positions of the deleted residues. (B) Responses of *Pvr9* to different internally deleted NIbs (NIbΔ(186–235), NIbΔ(236–369), and NIbΔ(370–445)). (C) Representative structures of SMV–NIb hybrids that were made from SMV–NIb background and residues 186–235 and 370–445 from PepMoV–NIb; the numbers indicate the amino acid position in the PepMoV NIb sequence. (D) Response of *Pvr9* to different SMV–NIb hybrids. The responses (in A, B and D) were detected at 2 days after co-agroinfiltration by trypan Blue (TB, left panel, scale bar=200 μm) and DAB staining (DAB, right panel, scale bar=1 cm).

homolog 1 and PepMoV *NIb* in *N. benthamiana* did not elicit any response (clone H1, Fig. 7A). To find regions responsible for the loss-of-function, hybrids of *Pvr9* and *homolog 1* were generated. Via the restriction enzyme (RE) sites *Nhe*I and *Hpa*I in the coding sequence, Pvr9 protein was divided into three segments: from residue 1–261 (1–261); residue 262–680 (262–680); and residue 681–1298 (681–1298). Each segment was mutually exchanged between *Pvr9* and *homolog 1*, and the constructs were co-agroinfiltrated with PepMoV *NIb*. As shown in Fig. 7A, the replacement of segment 262–680 of Pvr9 with the corresponding segment of homolog 1 resulted in loss of Pvr9 function (clone 2a); in a mutual relationship, homolog 1 gained the function when it contained segment 262–680 from Pvr9 (clone 2b); the other exchanges did not cause loss-of-function in Pvr9 (clones 1a and 3a) or did not gain the function in homolog 1 (clones 1b and 3b). Compared to Pvr9, there were three amino acid changes in segment 262–680 of homolog 1: K384E, E492G, and A652T. To determine which change is responsible for the loss-of-function, we generated single mutants at residue 384 from K to E, at residue 492 from E to G, or at residue 652 from A to T; only the mutation at residue 492 caused the loss-of-function (Fig. 7B, clone E492G). To investigate the function of residue 492, substitutions E492D, E492K, E492Q, and E492P were made; all of these mutants lost the function (Supplementary Fig. S3). Non-reciprocally, the substitution of the corresponding G492 to E in homolog 1 did not recover the function (clone H1-G492E); however, double mutagenesis revealed that the double mutant with G492E and T492A was completely functional (Fig. 7B, clone H1 G492E-T492A). To investigate the possible function of residue 652 in Pvr9, A652 was replaced by L, G, or P; the mutations at residue 652 did not prevent Pvr9 from responding to *NIb* but did reduce the response (i.e., it reduced the number of hypersensitive spots per total infiltrated spots) (Supplementary Fig. S4).

From the PepMoV resistant cultivar CM334, a genomic homologous sequence of *Pvr9* was isolated and named *homolog 2*. The putative amino acid alignment showed that homolog 2 had an insertion of six amino acids between residues 6 and 7, an insertion of three amino acids between residue 243 and 244, and 25 substitutions (Supplementary Fig. S2). As was the case with *homolog 1*, co-agroinfiltration of *homolog 2* and PepMoV *NIb* in *N. benthamiana* did not elicit any response (clone H2, Fig. 7C). To investigate the region responsible for the loss-of-function, we generated several swapped clones (Fig. 7C) via the RE sites *Nhe*I and *Hpa*I or via overlap extension PCR. As shown in Fig. 7C, only the exchange of segment 681–1298 caused loss-of-function in Pvr9 and gain-of-function in homolog *2* (clones 6a and 6b); the other exchanges did not alter the function of Pvr9 (clones 4a and 5a) and homolog *2* (clones 4b and 5b). To narrow the search region, we generated additional swapped clones by overlap extension PCR (Fig. 7C); the exchanges of segment 681–735 and segment 1045–1298 caused loss of Pvr9 function (clones 7a and 9a) while the exchange of segment 735–1045 did not (clone 8a); however, none of these segment replacements resulted in gain-of-function in homolog 2. These results suggested that two or more

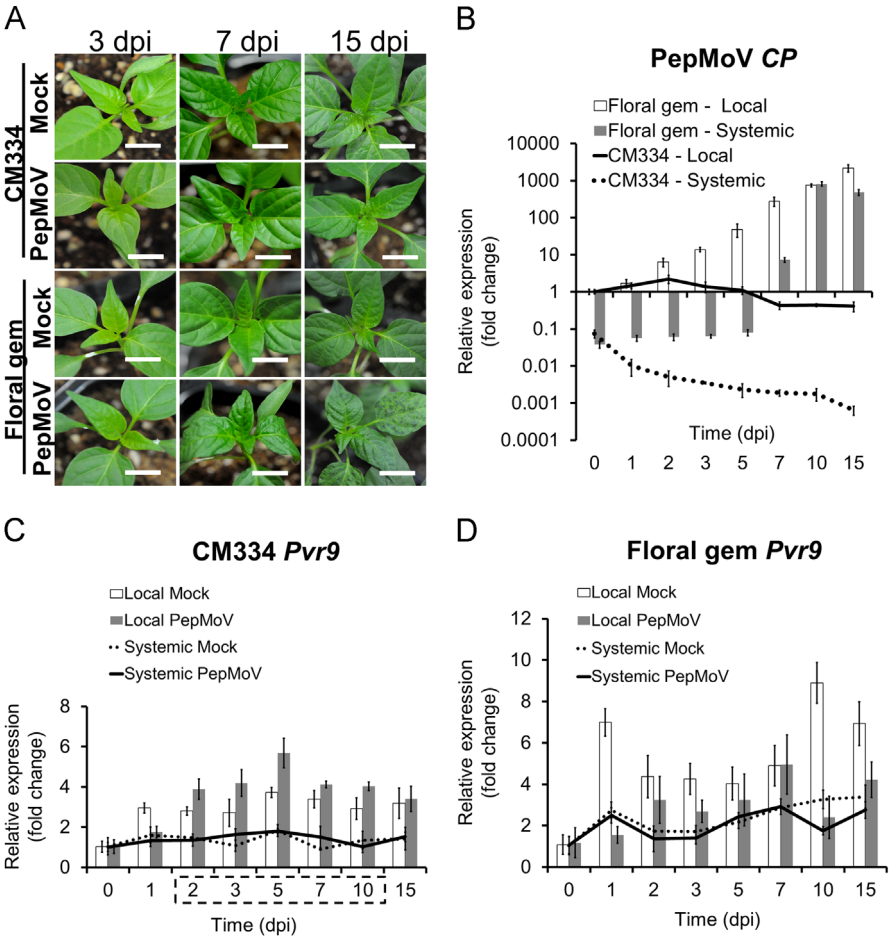

Fig. 5. PepMoV infectivity and Pvr9 expression profiles in peppers. (A) Symptoms of pepper cultivars CM334 and Floral Gem at 3, 7, and 15 days after inoculation (dpi) with PepMoV (PepMoV) or mock (Mock); scale bars=2 cm. (B) Replication of PepMoV in the inoculated leaves (Local) and upper leaves (Systemic) of pepper cultivars CM334 (line graphs) and Floral Gem (column graphs) was expressed as relative expression (fold change) of PepMoV CP in comparison to samples collected before inoculation. (C and D) Relative expression of *Pvr9* in inoculated leaves (Local, columns graphs) and upper leaves (Systemic, line graphs) of pepper cultivars CM334 and Floral Gem following mock and PepMoV inoculation and in comparison to the sample collected before inoculation (at 0 dpi). The error bars (B–D) indicate ±SD (standard deviation) of biological triplicates. The dashed box (in C) indicates time points with significant increasing of *Pvr9* transcription of PepMoV inoculated leaves in comparison to the mock inoculated ones.

amino acid substitutions independently cause the loss-of-function in homolog *2*. Compared to Pvr9 amino acid sequence, homolog 2 had one substitution in segment 681–735 (V701E) and eight substitutions in segment 1045–1298 (V1066E, V1089D, F1117S, R1160K, I1288V, Q1291R, E1292H, and D1293N). Among them, substitutions I1288V, Q1291R, E1292H, and D1293N are also present in the C terminus of homolog 1, which functioned normally in several chimera clones (Figs. 7A, 2b and 3a). We therefore made and investigated only five single-point mutants from Pvr9 including V701E, V1066E, V1089D, F1117S, and R1160K. As shown in Fig. 7D, the point mutants V701E, F1117S, and R1160K led to the loss of Pvr9 function while the others did not; the function of homolog 2 was completely recovered in the triple mutant with E701V, S1117F, and K1160R (clone H2 E701V-S1117F-K1160R).

Discussion

Resistance genes in plants are usually present in clusters of tightly linked genes (Hulbert et al., 2001). In CM334 pepper, two dominant potyvirus resistance genes, *Pvr4* and *Pvr7*, are tightly linked and located on chromosome 10 (Grube et al., 2000). The *Pvr9* gene characterized in this study was not related to those *R* genes but might be linked to another dominant potyvirus *R* gene, *CVMV*, which was recently mapped on chromosome 6 of *C. annuum* "NW4" (Lee et al., 2013). That both *Pvr9* and *CVMV* were found between the markers C2At2g39690 and C2At3g25120 in the short arm of chromosome 6 also suggested that the genes may be linked. Because the distance between the two markers was large (around 7.5 mega base pairs), however, additional research is needed to elucidate the relationship between *Pvr9* and *CVMV*.

Genome-wide analyses have revealed that *R* genes are very diverse and abundant in plant genomes (Kohler et al., 2008; Meyers et al., 2003; Zhou et al., 2004). Recently, the whole genome sequencing and assembly of the pepper *C. annuum* 'CM334' has been reported; 684*R* gene coding sequences were predicted in the pepper genome (Kim et al., 2014). *Pvr9* was previously cloned from a genomic DNA of the pepper *C. annuum* 'Floral Gem' based on sequence homology (Tran et al., 2014). This *R* gene isolation strategy could detect *R* genes whose functions are not expressed in the original host but can be expressed in other plants. This is the case with *Pvr9*, which was isolated from a PepMoV-susceptible pepper but which conferred resistance to PepMoV in *N. benthamiana*. *Pvr9* did not respond to PepMoV in pepper probably because an unknown factor that mediates the recognition of PepMoV NIb by Pvr9 protein is lacking in pepper. The failure to detect a direct

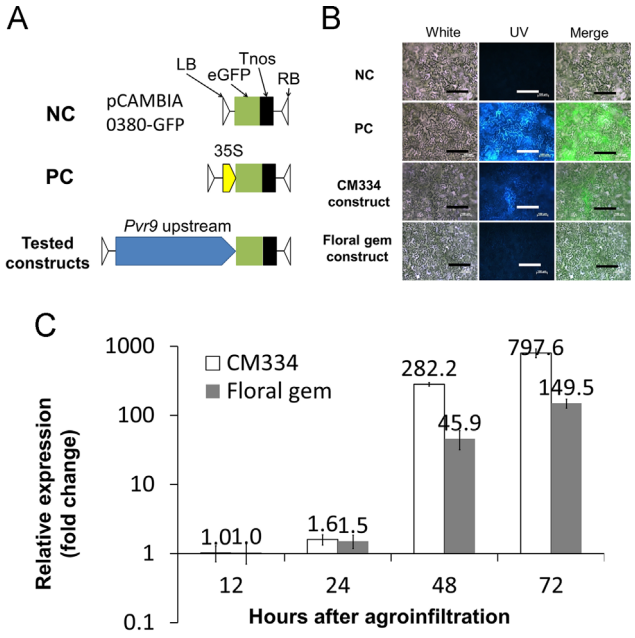

Fig. 6. Promoter activity of upstream sequences of *Pvr9*. (A) Representative structures of transient expression vectors for promoter activity assay. The clones of negative control, positive control and *Pvr9* upstream sequences were indicated as NC, PC and tested constructs For the construction of a negative control clone (NC), eGFP was fused to the upstream of the Tnos terminator (Tnos) and between the left border (LB) and right border (RB) of the binary promoterless vector pCAMBIA0380. For the construction of a positive control clone (PC), the 35S promoter was cloned to the 5′ end of eGFP of the NC clone. For determination of promoter activity of upstream sequences, the 10.3-kb upstream sequences of *Pvr9* were constructed in the same way as the PC clone. (B) GFP signal of the negative controls, positive controls, and *Pvr9* upstream sequences from pepper cultivars CM334 (CM334 construct) and Floral Gem (Floral Gem construct) as indicated by fluorescent microscopy; scale bars = 200 μm. (C) GFP transcription levels driven by *Pvr9* upstream sequences as determined by real-time RT-PCR. The samples were collected at 12, 24, 48, and 72 h after agroinfiltration. The number above each column indicates the relative expression of GFP (fold change) in comparison to the samples collected at 12 h after agroinfiltration. The error bars indicate ± SD of biological triplicates.

interaction between the *R* gene and the elicitor suggested that a third factor is present in *N. benthamiana* but does not in peppers. Since neither homolog 1 from Floral Gem nor homolog 2 from CM334 is capable of inducing hypersensitivity, it is also worth noting that the homolog 1 is probably an allelic variant of Pvr9 in the pepper Floral Gem population. How the *Pvr9* homologs present or evolve in the pepper Floral Gem as well as in the other cultivars remained to be clarified. As complete genome sequencing often identifies numerous allelic variants (sometimes hundreds) for a given gene, further study will determine significance of the genotype and corresponding phenotype using a sufficiently large population.

The fact that the homolog 2 from the CM334 cultivar was not functional indicated that *Pvr9* is not necessary to the *Pvr4* harboring pepper. However, the *Pvr9* transcription patterns seemed to link with susceptibility to the virus. The promoter activity driven by the *Pvr9* upstream sequence may contribute to the differences of *Pvr9* transcription in both cultivars. In that case, *Pvr9* could be one auxiliary component that is up-regulated when resistance blocks virus infection and down-regulated by the successful virus infection. The possible regulatory mechanisms of *Pvr9* expression remain to be clarified.

Avirulence factors of viral plant pathogens usually act as elicitors of resistance conferred by *R* genes but can also act as virulence factors. For example, the helicase domain triggers the *N* gene-mediated hypersensitive response to the TMV U1 strain but also enables the TMV Ob strain to overcome the resistance (Abbink et al., 2001). The CP elicits the hypersensitive response of *Rx*-transgenic tobacco to PVX but also carries the resistance-breaking determinant in PVX strain HB (Querci et al., 1995). Several potyvirus proteins have been proven to be elicitors of resistance or determinants of avirulence with respect to dominant resistance genes in plants. For example, TuMV CI is an avirulence factor of oilseed rape R genes *TufB01* (Jenner et al., 2000); SMV P3 and HC are elicitors of the soybean *R* gene *Rsv-1* (Eggenberger et al., 2008); and PVY NIa is the elicitor of potato *R* gene *Ry* (Mestre et al., 2000). As reported by Janzac et al., a mutation in the NIb of PVY confers virulence toward the *Pvr4*-based resistance of pepper and a high competitiveness cost in the susceptible cultivar (Janzac et al., 2010). In terms of a gene-for-gene relationship, this NIb could be an avirulence factor that is recognized by genotypes of the host plants that harbor the matching resistance gene. The elicitor characteristic of NIb in our study supported the likelihood that NIb is a novel avirulence determinant of potyvirus resistance. The *Pvr9* response elicitation activity of NIbs seems relatively conserved among the potyviruses. The intensity of the responses of Pvr9 to different NIbs (in terms of TB and DAB staining) was positively correlated with the similarity of the potyvirus NIb to PepMoV NIb. This suggested that the weak or non-elicitation ability of ZYMV NIb and SMV NIb is due to a weak phylogenetic relationship between these NIbs and PepMoV NIb. Responses of *Pvr9* to truncated and internally deleted PepMoV *NIb* constructs demonstrated that at least two internal sequences are responsible for the elicitor activity of the NIb protein. This activity was recovered in SMV NIb by replacement of the corresponding regions from PepMoV NIb. Further point mutation analyses in PepMoV NIb should be made for dissection of its elicitor activity. Given that NIb is an avirulence factor; these two regions could be important to viral pathogenicity. This hypothesis should be tested in the future.

From the CM334 and Floral Gem pepper cultivars, we identified two *Pvr9* homologs that are no longer capable of conferring a NIb-elicited hypersensitive response. The amino acid substitutions E492G, V701E, F1117S, and R1160K were determined to cause the loss of Pvr9 function. The substitution E492G in the possible CC domain of homolog 1 lies between a possible leucine zipper and a heptad repeat (Supplementary Fig. S2). In the Rx protein, the CC domain interacts with NBS-LRR moieties in pathogen recognition and signaling (Rairdan et al., 2008). The CC domain is also important in pathogen recognition in "guard" model. For example, the CC domains of NBS-LRR proteins RPM1 and RPS2 interact with *Arabidopsis* RIN4 protein during recognition of the *Pseudomonas syringae* type III effectors (Mackey et al., 2002); AvrRpt2 interacts with *Arabidopsis* PBS1 kinase, which binds to the CC domain of NBS-LRR protein RPS5 (Shao et al., 2003). Any of five point mutations at residue 492 caused loss of Pvr9 function indicated that this residue is critical. These substitutions could disrupt the interaction between domains of Pvr9 or/and compromise the downstream signaling.

In addition to residue E492, homolog 1 carries a substitution A652T at corresponding residue 652 of Pvr9; the reversion from T to A is necessary for the functional recovery of this homolog; however, the mutation A652T did not prevent *Pvr9* from conferring the hypersensitive response to PepMoV *NIb*. As described above, the comparison between Pvr9 and homolog 1 revealed one insertion and 16 substitutions; this suggested that another residue (s) might functionally compensate for the role of residue 652 in the Pvr9 background. This hypothesis will need to be tested in further mutagenesis analyses.

The third substitution V701E which was found in homolog 2 is adjacent to a putative kinase-3a motif (Supplementary Fig. S2, V701E; Fig 9D, clone V701E). Previously published mutation

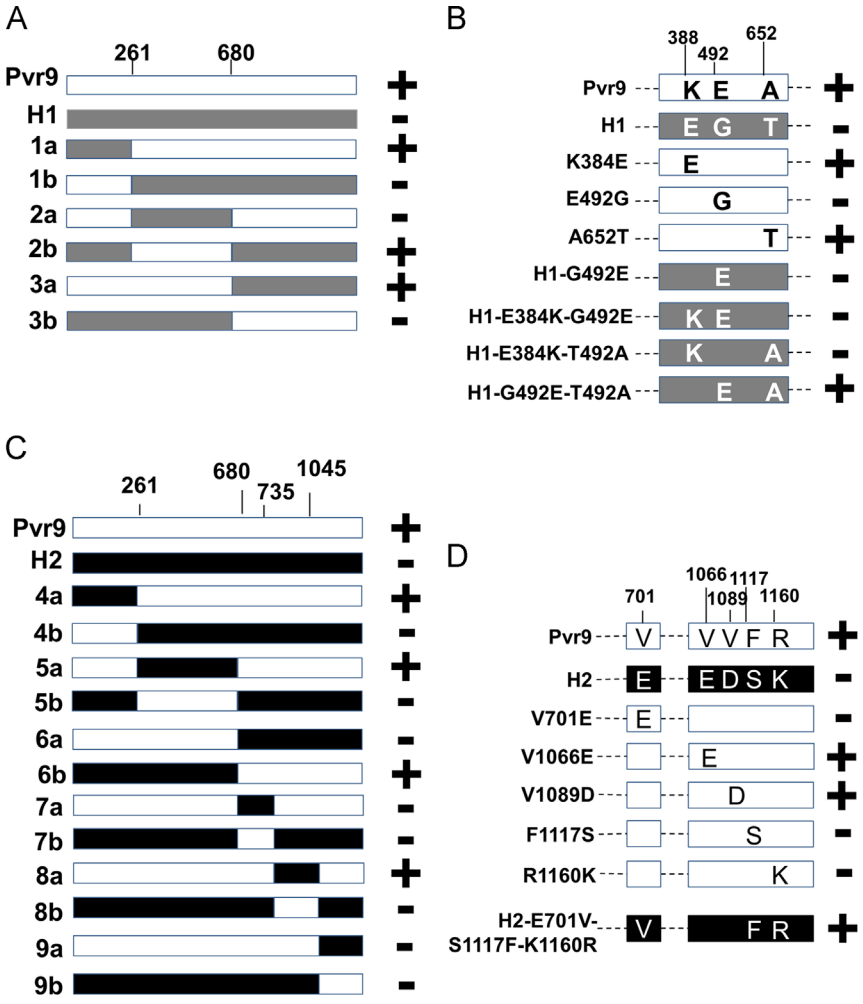

Fig. 7. Mutational analyses of Pvr9 and homologs. Responses of *Pvr9*, the homologs, and mutants were determined by co-agroinfiltration with PepMoV *NIbs*. The presence or absence of a hypersensitive response in each of the constructs is indicated by plus (+) or minus (−) signs. (A) Swapped constructs were made from Pvr9 and homolog 1 (H1) by exchange of the N terminal fragment (1a and 1b), the central fragment (2a and 2b), and the C terminal fragment (3a and 3b) of the proteins. (B) Point mutations at the central region of Pvr9 include K384E, E492G, and A652T. The C terminal point mutants derived from homolog 1 include H1-G492E, H1-E384K-G492E, H1-E384K-T492A, and H1-G492E-T652A. (C) Swapped constructs were made from *Pvr9* and *homolog 2* by exchange of the N terminal fragment (4a and 4b), the central fragment (5a and 5b), and the C terminal fragment (6a and 6b) of the proteins. The C terminals of Pvr9 and homolog 2 were then analyzed by additional swapped constructs (7a and 7b, 8a and 8b, 9a and 9b). (D) Point mutations at the C terminal region of Pvr9 include V701E, V1066E, V1089D, F1117S, and R1160K. The triple mutant of homolog 2 simultaneously contains the mutations E701V, S1117F, and K1160R (as H2-E701V-S1117F-K1160R).

analyses of *R* genes identified many amino acid substitutions in the NBS-ARC domain that compromise ATP/GFP binding/hydrolysis activity and lead to the loss-of-function (Takken et al., 2006). The hhhhToR signature (h is a mostly hydrophobic residue, and o is an alcoholic residue) in kinase-3a corresponds to the sensor I motif in AAA+ATPases and functions in γ-phosphate sensing (Iyer et al., 2004; Ogura and Wilkinson, 2001). Further research is required to determine whether the V701E substitution affects this sensing activity.

The substitutions F1117S and R1160K in the LRR domain of homolog 2 could interfere with interactions between this domain and the NIb target. The LRR domain contains the protein recognition motifs LxxLxLxxNxL which appear to provide a versatile structural framework for the formation of protein–protein interactions (Kobe and Kajava, 2001). R1160K is especially within one of the LxxLxLxxNxL repeats. LRR domain of R genes interacts directly (Deslandes et al., 2003; Dodds et al., 2006; Krasileva et al., 2010) or indirectly (Axtell and Staskawicz, 2003; Mackey et al., 2003, 2002) with pathogen effectors. In many plant R proteins, this domain is also thought to have co-evolved with pathogen effectors (Dodds et al., 2006; Ellis et al., 2000). The mechanism of the proposed indirect interaction between Pvr9 and NIb is unclear.

Materials and methods

Plant materials and virus inoculum

C. annuum Floral Gem and *C. annuum* CM334 were used for observation of gene expression as well as for isolation of *Pvr9* homologs and *Pvr9* upstream sequences. *N. benthamiana* was used for *Agrobacterium*-based transient expression of *Pvr9* constructs, viral genes, and promoter constructs. PepMoV isolate 134 was maintained in *N. benthamiana*; extraction of viral sap and inoculation were described previously (Tran et al., 2014).

Cloning and mutagenesis

To identify the coding sequence of *Pvr9*, total RNAs were extracted with Isol-RNA lysis reagent (5Prime) from *Pvr9* agroinfiltrated leaves at 2 days after agroinfiltration. The total RNAs were then treated with RQ1 DNase I (Promega) to remove DNA contamination. Double-stranded cDNA of *Pvr9* was amplified by RT-PCR with primers 1 and 2 (Supplementary Table 1) using GoScript reverse transcriptase (Promega) and EX *taq* DNA polymerase (Takara). The PCR product was ligated to the pGEM Teasy vector

(Promega) using *T4* DNA ligase (Promega). The sequence of the *Pvr9* cDNA clone was checked by sequencing with M13 primers and *Pvr9*-specific primers (Supplementary Table 1, primers 3–8). The *Pvr9* cDNA clone was then digested by *Mlu*I and ligated to the modified pPZP212 vector (Park et al., 2009).

The outermost 5′and 3′ genomic sequences of *Pvr9* in pepper were identified by chromosome walking as described previously (Reddy et al., 2008). First, total genomic DNA was extracted from leaves of pepper cultivars CM334 and Floral Gem with the DNeasy Plant Mini Kit (Qiagen). Strand-displacement reactions were then conducted using *phi29* DNA polymerase (NEB) and walker adaptors (Supplementary Table 1, no. 9–12). Finally, chromosome walking reactions were carried out by nested PCRs with walker primers and locus-specific primers (Supplementary Table 1, primers 13–18). Sequences of the PCR products were checked by sequencing with locus-specific primers.

To isolate homologous genomic *Pvr9* sequences from various pepper genotypes, PCR amplifications were conducted with primers designed from the chromosome walking (Supplementary Table 1, primers 19–20) using genomic total DNAs as templates. The PCR products were cloned to the pGEM-T Easy vector and confirmed by the same procedure used for *Pvr9*. The *Pvr9* homologs were then transferred from the pGEM-T easy vector to the modified pPZP212 via the *Mlu*I RE site.

To identify the upstream sequences of *Pvr9*, full *Pvr9* with identified outermost sequences was blasted against the pepper genome database (http://cab.pepper.snu.ac.kr/). A highly homologous sequence (> 99.7% identity to *Pvr9*) of 5574 base-pairs upstream of *Pvr9* was found in scaffold4966 (total 11,394 base pairs) of pepper scaffold database version 1.1. The 5574 base pairs were then found (100% identical) in counter-orientation from nucleotide 223206 to nucleotide 217,633 in scaffold1553 (total 558,846 base-pairs) of pepper scaffold database version 1.2. From this scaffold, three overlapped fragments upstream of *Pvr9* (3872, 3537, and 3798 base pairs) were amplified with specific primers (Supplementary Table 1, primers 21–26) and stepwise cloned to the pGEM-T easy vector via TA cloning, *Nhe*I/*Sac*I, and *Sac*I RE sites. Plasmids of transformants were confirmed by sequencing with specific primers (Supplementary Table 1, primers 27–38). The united 10,348 base pair upstream sequences were then digested by *Sac*II, end-blunted by Klenow fragment (Takara), and ligated to the modified promoterless vector GFP-pCAMBIA0380 by blunt-end ligation using T4 ligase.

To identify and characterize the elicitor of *Pvr9*, ten genes of PepMoV isolate 134 (EU586123) were amplified by RT-PCR from total RNAs of PepMoV-infected tissue using the viral gene flanking primers (Supplementary Table 1, primers 39–58) with fused start codons at the 5′ends; based on ribosomal frameshifting motif (Chung et al., 2008), P3N-PIPO coding sequence was made by fusion of N terminal coding sequence of P3 protein and PIPO coding sequence (Supplementary Table 1, primers 43, 59–61). *NIbs* from PVY, PVA, TuMV, ZYMV, and SMV were amplified by RT-PCR with the flanking primers (Supplementary Table 1, primers 62–71) using total RNA from the virus-infected tissues. The truncated in-frame PepMoV *NIbs* were amplified from full-length PepMoV *NIb* with PepMoV *NIb* outermost primers and internal primers (Supplementary Table 1, primers 72–75). To make internally deleted PepMoV *NIbs*, small DNA segments were made by PCRs with PepMoV outermost primers and overlapping primers (Supplementary Table 1, primers 76–81); final PCR products of internally deleted *NIbs* were made by overlap extension PCRs (Ho et al., 1989) from two short segments (Fig. 4B; segments a and b for NIbΔ(186–235), segments c and d for NIbΔ(236–369), segments e and f for NIbΔ(370–445)). To make SMV-PepMoV *NIb* hybrids, small PCR segments were amplified with SMV *NIb* outermost primers, SMV internal and overlapping primers (Supplementary Table 1, primers 82–89); overlapping PCRs were carried out from small segments (Fig. 5C; segments 1, 2, and 3 for hybrid 1; segments 4, 5, and 6 for hybrid 2; segments 1, 2, 7, 5, and 6 for hybrid 3). The *Mlu*I-digested PCR products of the non-mutated and mutated *NIbs* were cloned to the modified pPZP212 via the *Mlu*I RE site.

To make swapping constructs of *Pvr9*, *Pvr9* and *homologs* were first cloned to the pGEM-Teasy vector; the swapping of the N terminal region, central region, and C terminal region between *Pvr9* and *homologs* was carried out by restriction enzyme digestion (ligation via *Sac*I–*Nhe*I, *Nhe*I–*Hpa*I, and *Hpa*I–*Apa*I) or by overlap extension PCR with some *Pvr9* outermost primers and internal primers (Supplementary Table 1, primers 90–91). These swapped products were transferred from the pGEM-T easy vector to the modified pPZP212 via the *Mlu*I RE site.

To make point mutations for *Pvr9*, site-directed mutagenesis was carried out by overlap extension PCR (in Supplementary Table 1, primers 92–109 were used for comparative analysis of *Pvr9* and *homolog 1*, and primers 110–115 were used for the analysis of *Pvr9* and *homolog 2*). The mutants were transferred from the pGEM-T easy vector to the modified pPZP212 via the *Mlu*I RE site.

The nucleotide sequence of *Pvr9*, its homologs and upstream sequences were deposited into the gene bank NCBI, with following accession numbers:

- *Pvr9* with 10.3 kbps upstream sequence: KM590984
- *Homolog 1*: KM590985
- *Homolog 2* with 10.3 kbps upstream sequence: KM590986

Agroinfiltration and cell death detection

Agrobacterium tumefaciens GV3101 was used for all constructs in the modified pPZP212 vectors. Agroinfiltration was conducted as described previously (Tran et al., 2014). For detection of the hypersensitive response, infiltrated leaves were detached 2 days after agroinfiltration and were stained with 3,3′-diaminobenzidine (DAB) and trypan blue (TB) as described previously (Van Wees, 2008) with minor modifications. The infiltrated leaves and DAB-stained leaves were imaged with a digital camera (Nikon 7200). Differential interference contrast (DIC) images of TB-stained tissues were obtained with an Axio Imager A1 Microscope (Carl Zeiss Ltd.) and a 20 × -objective lens.

Real-time RT-PCR

For quantification of transcripts of PepMoV, plant genes, and transiently expressed genes, total RNAs were collected from pepper or tobacco leaves and treated with Dnase I (RQ1, Promega) to remove DNA contamination. Real-time PCR was then carried out with biological triplicates and three technical replicates in a LightCycler 480 instrument (Roche) using a qRT-PCR kit (PrimeScript, Takara) as described by the manufacturer. Reference amplifications of pepper GAPDH (Wan et al., 2011) and *N. benthamiana* F-box (Liu et al., 2012) were conducted with specific primers (Supplementary Table 1, primers 116–119). Primers specific to PepMoV CP (Supplementary Table 1, primers 120–121) were used for detection of PepMoV. Specific and exon–exon spanning primers were used for detection of *Pvr9* transcripts (Supplementary Table 1, primers 122–123). Primers specific to GFP (Supplementary Table 1, primers 124–125) were used to detect GFP transcripts. Ct values of target or reference genes were recorded with LightCycler 480 software (version 1.5) and were statistically calculated with Microsoft Excel 2010 software as previously described (Schmittgen, 2006).

Acknowledgments

This research was supported in part by grants from the Vegetable Breeding Research Center (No. 710001-07-5) through the Agriculture, Food and Rural Affairs Research Center Support Program from the Ministry of Agriculture, Food and Rural Affairs and the Next-Generation BioGreen 21 Program (No. PJ01101401), Rural Development Administration (RDA). PT and HC were supported by research fellowships from the Brain Korea 21 Plus Project.

Appendix A. Supporting information

Supplementary data associated with this article can be found in the online version at http://dx.doi.org/10.1016/j.virol.2015.02.052.

References

Abbink, T.E., de Vogel, J., Bol, J.F., Linthorst, H.J., 2001. Induction of a hypersensitive response by chimeric helicase sequences of tobamoviruses U1 and Ob in N-carrying tobacco. Mol. Plant-Microbe Interact. 14, 1086–1095.

Andrés, A., Luis Arteaga, M., Gil Ortega, R., Voorrips, R., 2004. New genes related to PVY resistance in *C. annuum* L.'Serrano Criollo de Morelos-334'. In: Proceedings of the XIIth EUCARPIA meeting on genetics and breeding of Capsicum and eggplant, Noordwijkerhout, Netherlands, 17–19 May, 2004. European Association for Research on Plant Breeding (EUCARPIA), pp. 134–138.

Axtell, M.J., Staskawicz, B.J., 2003. Initiation of *RPS2*-specified disease resistance in *Arabidopsis* is coupled to the AvrRpt2-directed elimination of *RIN4*. Cell 112, 369–377.

Bej, A., Sahoo, B.R., Swain, B., Basu, M., Jayasankar, P., Samanta, M., 2014. LRRsearch: an asynchronous server-based application for the prediction of leucine-rich repeat motifs and an integrative database of NOD-like receptor. Comput. Biol. Med. 53, 164–170.

Caranta, C., Lefebvre, V., Palloix, A., 1997. Polygenic resistance of pepper to potyviruses consists of a combination of isolate-specific and broad-spectrum quantitative trait loci. Mol. Plant-Microbe Interact. 10, 872–878.

Caranta, C., Palloix, A., Gebre-Selassie, K., Lefebvre, V., Moury, B., Daubeze, A., 1996. A complementation of two genes originating from susceptible *Capsicum annuum* lines confers a new and complete resistance to pepper veinal mottle virus. Phytopathology 86, 739–743.

Chisholm, S.T., Coaker, G., Day, B., Staskawicz, B.J., 2006. Host–microbe interactions: shaping the evolution of the plant immune response. Cell 124, 803–814.

Chung, B.Y.-W., Miller, W.A., Atkins, J.F., Firth, A.E., 2008. An overlapping essential gene in the Potyviridae. Proc. Natl. Acad. Sci. USA 105, 5897–5902.

Cook, A., 1960. A mutation for resistance to potato virus Y in pepper. Phytopathology 50, 632.

Cook, A., Anderson, C., 1959. Multible virus disease resistance in a strain of *Capsicum annuum*. Phytopathology 49, 198–201.

Dangl, J.L., Jones, J.D., 2001. Plant pathogens and integrated defence responses to infection. Nature 411, 826–833.

Deslandes, L., Olivier, J., Peeters, N., Feng, D.X., Khounlotham, M., Boucher, C., Somssich, I., Genin, S., Marco, Y., 2003. Physical interaction between RRS1-R, a protein conferring resistance to bacterial wilt, and PopP2, a type III effector targeted to the plant nucleus. Proc. Natl. Acad. Sci. USA 100, 8024–8029.

Diaz-Pendon, J.A., Truniger, V., Nieto, C., Garcia-Mas, J., Bendahmane, A., Aranda, M.A., 2004. Advances in understanding recessive resistance to plant viruses. Mol. Plant Pathol. 5, 223–233.

Dodds, P.N., Lawrence, G.J., Catanzariti, A.-M., Teh, T., Wang, C.-I., Ayliffe, M.A., Kobe, B., Ellis, J.G., 2006. Direct protein interaction underlies gene-for-gene specificity and coevolution of the flax resistance genes and flax rust avirulence genes. Proc. Natl. Acad. Sci. USA 103, 8888–8893.

Dogimont, C., Palloix, A., Daubze, A.-M., Marchoux, G., Selassie, K.G., Pochard, E., 1996. Genetic analysis of broad spectrum resistance to potyviruses using doubled haploid lines of pepper (*Capsicum annuum* L.). Euphytica 88, 231–239.

Eggenberger, A., Hajimorad, M., Hill, J., 2008. Gain of virulence on *Rsv1*-genotype soybean by an avirulent *Soybean mosaic virus* requires concurrent mutations in both P3 and HC-Pro. Mol. Plant-Microbe Interact. 21, 931–936.

Ellis, J., Dodds, P., Pryor, T., 2000. Structure, function and evolution of plant disease resistance genes. Curr. Opin. Plant Biol. 3, 278–284.

Ellis, J.G., Dodds, P.N., Lawrence, G.J., 2007. Flax rust resistance gene specificity is based on direct resistance–avirulence protein interactions. Annu. Rev. Phytopathol. 45, 289–306.

Gebre Selassie, K., Marchoux, G., Pochard, E., 1983. Biological and serological characterization of potato virus Y strains affecting peppers and other related strains. Capsicum Newsl. 2, 134–136.

Greenleaf, W., 1956. Inheritance of resistance to tobacco etch virus in Capsicum frutescens and in *Capsicum annuum*. Phytopathology 46, 371–375.

Greenleaf, W., 1986. Pepper breeding. Breed. Veg. Crops 6880, 67–133.

Grube, R., Blauth, J., Andrés, M.A., Caranta, C., Jahn, M., 2000. Identification and comparative mapping of a dominant potyvirus resistance gene cluster in *Capsicum*. Theor. Appl. Genet. 101, 852–859.

Ho, S.N., Hunt, H.D., Horton, R.M., Pullen, J.K., Pease, L.R., 1989. Site-directed mutagenesis by overlap extension using the polymerase chain reaction. Gene 77, 51–59.

Hulbert, S.H., Webb, C.A., Smith, S.M., Sun, Q., 2001. Resistance gene complexes: evolution and utilization. Annu. Rev. Phytopathol. 39, 285–312.

Iyer, L.M., Leipe, D.D., Koonin, E.V., Aravind, L., 2004. Evolutionary history and higher order classification of AAA+ATPases. J. Struct. Biol. 146, 11–31.

Janzac, B., Montarry, J., Palloix, A., Navaud, O., Moury, B., 2010. A point mutation in the polymerase of *Potato virus Y* confers virulence toward the *Pvr4* resistance of pepper and a high competitiveness cost in susceptible cultivar. Mol. Plant-Microbe Interact. 23, 823–830.

Jenner, C., Sanchez, F., Nettleship, S., Foster, G., Ponz, F., Walsh, J., 2000. The cylindrical inclusion gene of *Turnip mosaic virus* encodes a pathogenic determinant to the *Brassica* resistance gene *TuRB01*. Mol. Plant-Microbe Interact. 13, 1102–1108.

Jones, P., Binns, D., Chang, H.-Y., Fraser, M., Li, W., McAnulla, C., McWilliam, H., Maslen, J., Mitchell, A., Nuka, G., 2014. InterProScan 5: genome-scale protein function classification. Bioinformatics 30, 1236–1240.

Kang, B.-C., Yeam, I., Jahn, M.M., 2005. Genetics of plant virus resistance. Annu. Rev. Phytopathol. 43, 581–621.

Kim, S., Park, M., Yeom, S.-I., Kim, Y.-M., Lee, J.M., Lee, H.-A., Seo, E., Choi, J., Cheong, K., Kim, K.-T., et al., 2014. Genome sequence of the hot pepper provides insights into the evolution of pungency in Capsicum species. Nat. Genet. 46, 270–278.

Kim, Y.-J., Jonson, M.G., Choi, H.S., Ko, S.-J., Kim, K.-H., 2009. Molecular characterization of Korean *Pepper mottle virus* isolates and its relationship to symptom variations. Virus Res. 144, 83–88.

Kobe, B., Kajava, A.V., 2001. The leucine-rich repeat as a protein recognition motif. Curr. Opin. Plant Biol. 11, 725–732.

Kohler, A., Rinaldi, C., Duplessis, S., Baucher, M., Geelen, D., Duchaussoy, F., Meyers, B.C., Boerjan, W., Martin, F., 2008. Genome-wide identification of *NBS* resistance genes in *Populus trichocarpa*. Plant Mol. Biol. 66, 619–636.

Krasileva, K.V., Dahlbeck, D., Staskawicz, B.J., 2010. Activation of an *Arabidopsis* resistance protein is specified by the in planta association of its leucine-rich repeat domain with the cognate oomycete effector. Plant Cell 22, 2444–2458.

Kyle, M., Palloix, A., 1997. Proposed revision of nomenclature for potyvirusresistance genes in *Capsicum*. Euphytica 97, 183–188.

Lee, H.-R., You, H.J., Lee, Y.G., Kim, J., Kang, H.-J., Harn, C.H., B.-C., 2013. Development of a novel codominant molecular marker for chili veinal mottle virus resistance in *Capsicum annuum* L. Euphytica 193, 197–205.

Levine, A., Tenhaken, R., Dixon, R., Lamb, C., 1994. H_2O_2 from the oxidative burst orchestrates the plant hypersensitive disease resistance response. Cell 79, 583–593.

Liu, D., Shi, L., Han, C., Yu, J., Li, D., Zhang, Y., 2012. Validation of reference genes for gene expression studies in virus-infected *Nicotiana benthamiana* using quantitative real-time PCR. PLoS One 7, e46451.

Mackey, D., Belkhadir, Y., Alonso, J.M., Ecker, J.R., Dangl, J.L., 2003. *Arabidopsis* RIN4 is a target of the type III virulence effector AvrRpt2 and modulates *RPS2*-mediated resistance. Cell 112, 379–389.

Mackey, D., Holt III, B.F., Wiig, A., Dangl, J.L., 2002. RIN4 interacts with *Pseudomonas syringae* type III effector molecules and is required for *RPM1*-mediated resistance in *Arabidopsis*. Cell 108, 743–754.

Mestre, P., Brigneti, G., Baulcombe, D.C., 2000. An *Ry*-mediated resistance response in potato requires the intact active site of the NIa proteinase from *Potato virus Y*. Plant J. 23, 653–661.

Meyers, B.C., Kozik, A., Griego, A., Kuang, H., Michelmore, R.W., 2003. Genome-wide analysis of NBS-LRR–encoding genes in *Arabidopsis*. Plant Cell 15, 809–834.

Moury, B., Palloix, A., Caranta, C., Gognalons, P., Souche, S., Selassie, K.G., Marchoux, G., 2005. Serological, molecular, and pathotype diversity of *Pepper veinal mottle virus* and *Chili veinal mottle virus*. Phytopatholoy 95, 227–232.

Murphy, J.F., Blauth, J.R., Livingstone, K.D., Lackney, V.K., Jahn, M.K., 1998. Genetic mapping of the pvr1 locus in Capsicum spp. and evidence that distinct potyvirus resistance loci control responses that differ at the whole plant and cellular levels. Mol. Plant-Microbe Interact. 11, 943–951.

Nelson, M., Wheeler, R., 1978. Biological and serological characterization and separation of potyviruses that infect peppers. Phytopathology 68, 979–984.

Ogura, T., Wilkinson, A.J., 2001. AAA+superfamily ATPases: common structure–diverse function. Genes Cells 6, 575–597.

Park, M.-R., Park, S.-H., Cho, S.-Y., Kim, K.-H., 2009. *Nicotiana benthamiana* protein, NbPCIP1, interacting with *Potato virus X* coat protein plays a role as susceptible factor for viral infection. Virology 386, 257–269.

Querci, M., Baulcombe, D., Goldbach, R., Salazar, L., 1995. Analysis of the resistance-breaking determinants of *Potato virus X* (PVX) strain HB on different potato genotypes expressing extreme resistance to PVX. Phytopathology 85, 1003–1010.

Rairdan, G.J., Collier, S.M., Sacco, M.A., Baldwin, T.T., Boettrich, T., Moffett, P., 2008. The coiled-coil and nucleotide binding domains of the potato Rx disease resistance protein function in pathogen recognition and signaling. Plant Cell 20, 739–751.

Rairdan, G.J., Moffett, P., 2006. Distinct domains in the ARC region of the potato resistance protein Rx mediate LRR binding and inhibition of activation. Plant Cell 18, 2082–2093.

Reddy, P.S., Mahanty, S., Kaul, T., Nair, S., Sopory, S.K., Reddy, M.K., 2008. A high-throughput genome-walking method and its use for cloning unknown flanking sequences. Anal. Biochem. 381, 248–253.
Schmittgen, T.D., 2006. Quantitative gene expression by real-time PCR: a complete protocol. In: Dorak, M. (Ed.), Real-Time PCR. Bios Scientific Publishers, Oxfordshire, pp. 127–137.
Shao, F., Golstein, C., Ade, J., Stoutemyer, M., Dixon, J.E., Innes, R.W., 2003. Cleavage of *Arabidopsis* PBS1 by a bacterial type III effector. Science 301, 1230–1233.
Takken, F.L., Albrecht, M., Tameling, W.I., 2006. Resistance proteins: molecular switches of plant defence. Curr. Opin. Plant Biol. 9, 383–390.
Tameling, W.I., Elzinga, S.D., Darmin, P.S., Vossen, J.H., Takken, F.L., Haring, M.A., Cornelissen, B.J., 2002. The tomato *R* gene products I-2 and MI-1 are functional ATP binding proteins with ATPase activity. Plant Cell 14, 2929–2939.
Tran, P.-T., Choi, H., Kim, S.-B., Lee, H.-A., Choi, D., Kim, K.-H., 2014. A simple method for screening of plant NBS-LRR genes that confer a hypersensitive response to plant viruses and its application for screening candidate pepper genes against *Pepper mottle virus*. J. Virol. Methods 201, 57–64.
Van Wees, S., 2008. Phenotypic analysis of *Arabidopsis* mutants: trypan blue stain for fungi, oomycetes, and dead plant cells. Cold Spring Harb. Protoc. 3, 10.1101.
Wan, H., Yuan, W., Ruan, M., Ye, Q., Wang, R., Li, Z., Zhou, G., Yao, Z., Zhao, J., Liu, S., 2011. Identification of reference genes for reverse transcription quantitative real-time PCR normalization in pepper (*Capsicum annuum L.*). Biochem. Bioph. Res. Commun. 416, 24–30.
Wu, F., Eannetta, N.T., Xu, Y., Durrett, R., Mazourek, M., Jahn, M.M., Tanksley, S.D., 2009. A COSII genetic map of the pepper genome provides a detailed picture of synteny with tomato and new insights into recent chromosome evolution in the genus *Capsicum*. Theor. Appl. Genet. 118, 1279–1293.
Zhou, T., Wang, Y., Chen, J.-Q., Araki, H., Jing, Z., Jiang, K., Shen, J., Tian, D., 2004. Genome-wide identification of NBS genes in *japonica* rice reveals significant expansion of divergent non-TIR NBS-LRR genes. Mol. Genet. Genomics 271, 402–415.
Zitter, T., Cook, A., 1973. Inheritance of tolerance to a pepper virus in Florida. Phytopathology 63, 1211–1212.